# Characterization of a Nano-Oxide Layer in a Pseudo Spin Valve by Complex Magneto-Impedance Spectroscopy

W. C. Chien[1], T. Y. Peng[2], L. C. Hsieh[3], C. K. Lo[3], and Y. D. Yao[4]

[1]Department of Physics, National Chung Cheng University, Chia-Yi 62145, Taiwan, R.O.C.
[2]Department of Materials Science and Engineering, National Chiao Tung University, Hsinchu 30010, Taiwan, R.O.C.
[3]Electronics and Optoelectronics Research Laboratories, Industrial Technology Research Institute, Hsinchu 31040, Taiwan, R.O.C.
[4]Institute of Physics, Academia Sinica Taipei 11529, Taiwan, R.O.C.

**The ac properties of a pseudo spin valve (PSV) consisting of $NOL_{top}$/Co/Cu/Co/$Ni_{80}Fe_{20}$/$NOL_{bottom}$ with a top and bottom nano-oxide layer (NOL) were studied as functions of NOL and thickness, *d*, by magneto impedance spectroscopy. The NOLs were formed by natural oxidizing the top and bottom ferromagnetic or Ta layers *in situ*. The increase in the thickness of NOL resulting in the increment of effective capacitance caused the shift of roll-off frequency from low to high. The frequency dependence behavior of this $NOL_{top}$/PSV/$NOL_{bottom}$ system can be modeled by equivalent circuit theory. PSV with a different NOL structure can be checked by such a nondestructive analysis method.**

***Index Terms*—Magneto-capacitance, magneto-impedance, nano-oxide layer, pseudo spin valve, roll-off frequency.**

## I. Introduction

SINCE the discovery of the giant magneto resistance (GMR) effect in magnetic multilayers, the application of spin-related technology has progressed broadly and rapidly over the last decade [1]. Spintronics, which may contain a magnetic tunneling junction (MTJ) or a pseudo spin valve (PSV) [2], has been widely expected to play a central role in the future generation of spin technologies such as nonvolatile memory, pick-up heads, magnetic sensors, etc. According to the past report [3], the growth of PSV films on nano-oxide layers (NOLs) has led to an enhancement in GMR. A corresponding reduction in minimum film resistance by over 10% confirms that this enhancement originates from an increase in the mean free path of spin-polarized electrons due to the resultant of specular reflection at nano-oxide surfaces. However, the properties of NOL in PSV are hard to analyze by nondestructive means. It has recently been shown that impedance spectroscopy can provide evidence to identify interface characteristics by using equivalent circuit analysis [4]. Consequently, in this study we extend our recent work [5] to study the PSV with different thicknesses of NOL by means of a nondestructive method—magneto-impedance spectroscopy.

Impedance, $Z = R + iX$ in which $X = X_L - X_C$, of the PSV originates mainly from the inductance and capacitance of the device. Impedance was measured under the influence of an external magnetic field resulting in magneto-impedance (MI) response. The MI loop of the PSV and the corresponding behavior of each of the components of the MI, i.e., $|MZ|$, MR, and MX, have been carefully examined in some detail.

Digital Object Identifier 10.1109/TMAG.2006.879730

As usual, the MZ ratio is defined as $100\% \times (|\ MZ\ |_{AP} — |\ MZ\ |_P)/|\ MZ\ |_P$, where the subscript P (AP) stands for the parallel (antiparallel) magnetization orientation state of the PSV. The magnetoresistance ratio (MR) and magnetoreactance ratio (MX) are all defined similarly. In fact the whole system contains nonignorable parasitic inductance and capacitance from wires, and these terms have effect on the shift of resonant frequency. However, these sensing wires do not have any contribution to the MI, and cannot prevent us from analyzing general MI phenomena.

## II. Experiment

The PSVs with NOL of $NOL_{top}$/PSV/$NOL_{bottom}$/substrate were grown by e-gun evaporation on a thermally oxidized Si (100) wafer with size of 1 cm × 1 cm. The $NOL_{top}$ was oxidized Co, and $NOL_{bottom}$ was one of oxidized Py, Co, and Ta. The PSV was Co 3/Cu 4/Co 1/Py 3, where Py denotes $Ni_{80}Fe_{20}$ and all thicknesses shown in the bracket are given in nanometers. The base pressure of the growing chamber was lower than $5 \times 10^{-8}$ Torr, and during the growth, the pressure never exceeded $10^{-7}$ Torr. The $NOL_{top}$ was obtained by oxidizing the 3-nm Co layer, while the Py-$NOL_{bottom}$ ($d$) was formed by oxidizing the Py layer with $d$ varied from 0 to 1.5 nm. Another two types of $NOL_{bottom}$ were obtained by oxidized 1-nm Co or Ta under the Py of the PSV. The oxidization process was done *in situ* by passing $O_2$ at the pressure of $10^{-5}$ Torr for 10 min. The ac behavior was determined by using the HP4194 impedance analyzer together with a 16047D fixture and a two-point probe. The sensing voltage of $\pm 0.5$ V with frequency that ranged from 100 Hz to 1 MHz was given by the analyzer while doing measurement [6]. During the characterization, the ac sensing voltage and external applied field of up to $\pm 100$ Oe were applied along

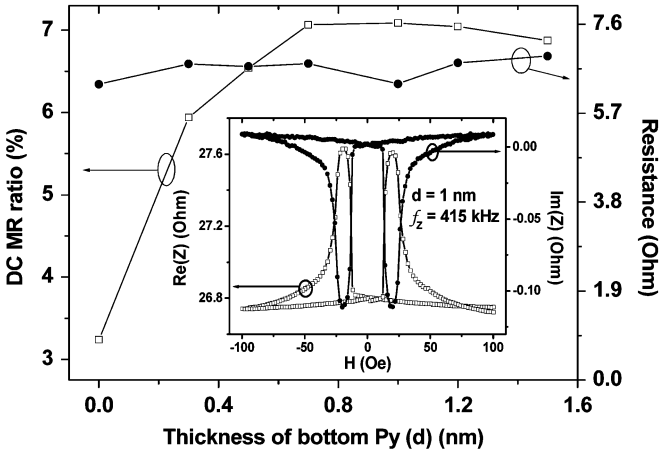


Fig. 1. Dependences on MR ratio, resistance, and thickness of the bottom Py in the structure of Ta 0.6/NOL/Co 3/Cu 4/Co 1/Py 3/NOL/Py (d)/substrate, in which the $\mathrm{NOL_{bottom}}$ Py was naturally oxidized for 10 min. The inset panel shows the magnetoimpedance at frequency 415 kHz for PSV with $d = 1$ nm. The shape of the $\mathrm{MZ_{Im}}$ loop is reversed to that of $\mathrm{MZ_{Re}}$.

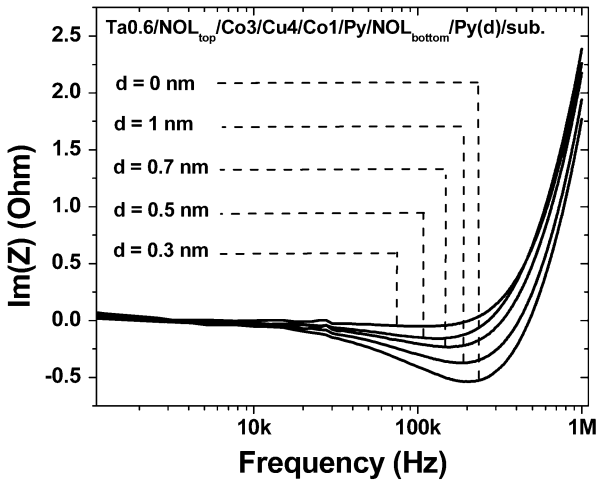


Fig. 2. Imaginary parts of impedance curves for PSV with different thicknesses of the Py $\mathrm{NOL_{bottom}}$ ranged from 0 to 1 nm at zero fields. Except the PSV without Py $\mathrm{NOL_{bottom}}$, the roll-off frequencies increase as the thickness of the Py $\mathrm{NOL_{bottom}}$ increases.

the easy axis of the PSV sample, i.e., longitudinal configuration was employed.

## III. Results and Discussions

Fig. 1 shows the resistance of the PSV as a function of the thickness of the Py-$\mathrm{NOL_{bottom}}$. The DC-MR increases rapidly from 3.2% at $d = 0$ and reaches to saturation of 7.1% at about 1 nm. That is, 1 nm of Py was thick enough to protect from oxidation. The inset panel in Fig. 1 shows the magnetoresistance (real part of MZ) and reactance (imaginary part of MZ) of the PSV with $d = 1$ nm at $f = 415$ kHz. The reverse loop of Im (MZ) with respect to that of the Re (MZ) means 90° out of phase, as expected. Note that it is impossible to distinguish effective capacitance and inductance of the $\mathrm{NOL_{top}}$/PSV/$\mathrm{NOL_{bottom}}$ from the impedance for the whole frequency spectrum; however, in our case, $X_C \gg X_L$, and hence $Z \approx R - iX_C$. We observed that magnetocapacitance, Im (MZ), at magnetically parallel state was larger than that at antiparallel state. This result was similar to that in [5] and [7].

The frequency and Py-$\mathrm{NOL_{bottom}}$ thickness dependences of Im (Z) at zero field for the $\mathrm{NOL_{bottom}}$ sample is shown in Fig. 2. Im (Z) reaches a minimum at roll-off frequency $(f_r)$. The plot of $f_r$ as a function of $d$ is shown in Fig. 3(a) that $f_r$ increases linearly before ~1 nm, and decreases afterward. While $d <$ 1 nm, the Py layers were fully oxidized, and the increment of Py would reduce the capacitance, hence the reduction of $f_r$ at thicker $d$. At $d > 1$ nm, the Py layers were not fully oxidized, and it cauased the increase of capacitance effect from a oxide-metal interface [8]. This result is consistent with the one shown in Fig. 1.

We used Maxwell–Wagner (M–W) model of capacitor consisting two dielectric materials [8] together with equivalent circuit (EC) theory to analysis our sample. The EC consists two parts, the $\mathrm{NOL_{top}}$/PSV/$\mathrm{NOL_{bottom}}$ and the sensing circuit as shown in Fig. 3 (b). In the first part, the circuit contains not only the resistance $(R_{\mathrm{NOL}})$ and capacitance $(C_{\mathrm{NOL}})$ from the NOL, but also has contributions from the interface, $R_{\mathrm{int}}$, and $C_{\mathrm{int}}$, respectively. In part two, the circuit components contain

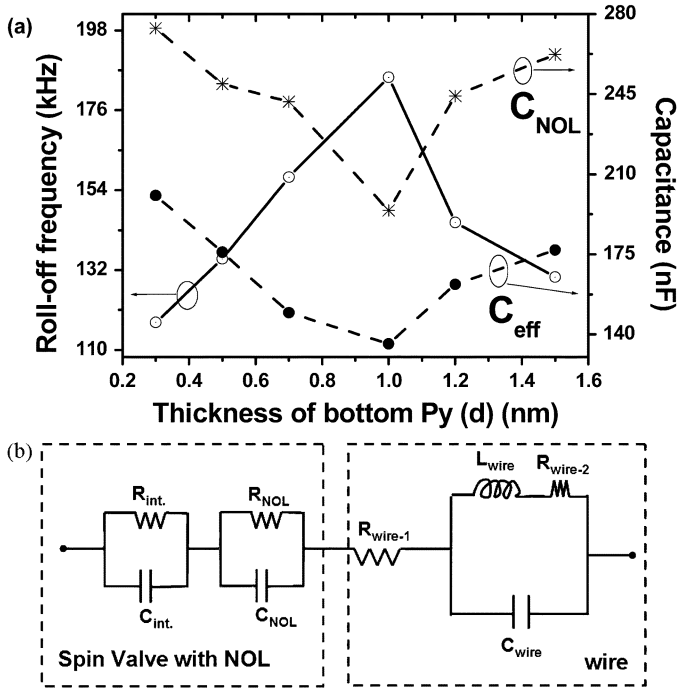


Fig. 3. (a) Roll-off frequency, the calculated effective, and the NOL capacitances are functions of the thickness of the Py $\mathrm{NOL_{bottom}}$ thickness. (b) The equivalent circuit of the measurement is a complex *RLC* combination.

resistor, capacitor, and an ignorable inductor; however, this part does not respond to the change of magnetic field. $f_r$ can be extracted from minimized $Z_{\mathrm{eff}}$

$$f_r = 1/(2\pi R_{\mathrm{eff}} C_{\mathrm{eff}}). \tag{1}$$

The behaviors of $f_r, C_{\mathrm{NOL}}$, and $C_{\mathrm{eff}}$ as $d$ is increased follow the M–W model and EC theory as shown in Fig. 3(a). Note that $R_{\mathrm{eff}}$ is also frequency dependent, which gives a maximum on inverse V-shape of $f_r$ versus $d$.

Fig. 4 shows the frequency dependence of the Im (Z) for the PSV with different NOL structures. The PSV with $\mathrm{NOL_{bottom}}$ of Ta1/Co3/Cu4.5/Co1

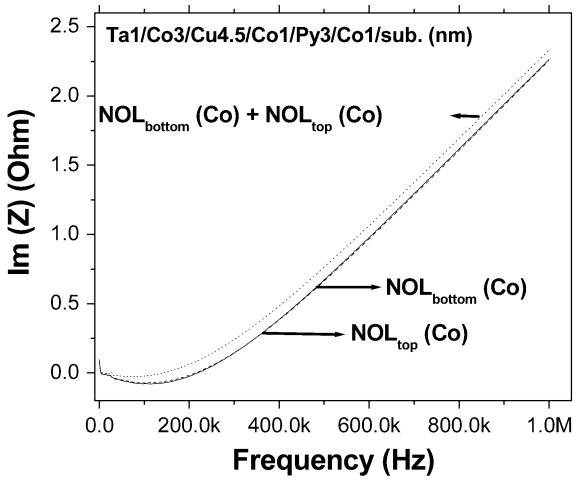


Fig. 4. Imaginary part of impedance curve for PSV with different NOL structures at zero fields. The film structure is Ta/(Co $\mathrm{NOL_{top}}$)/Cu/Co/Py/(Co $\mathrm{NOL_{bottom}}$)/sub.

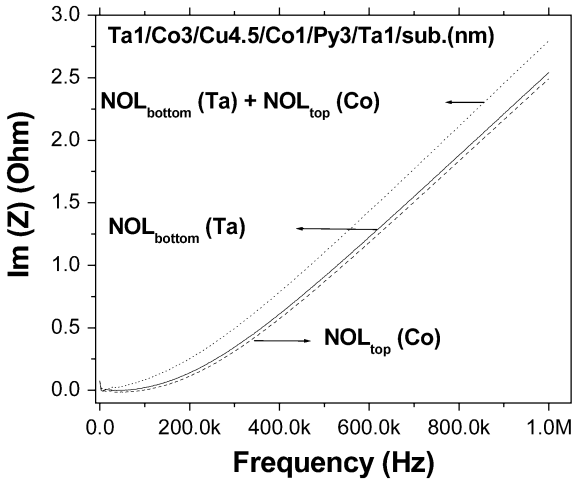


Fig. 5. Imaginary part of impedance curve for PSV with different NOL structures at zero fields. The film structure is Ta/(Co NOL)/Cu/Co/Py/(Ta NOL)/sub.

Py3/$\mathrm{NOL_{bottom}}$/Co1/substrate and the PSV with $\mathrm{NOL_{top}}$ of Ta1/$\mathrm{NOL_{top}}$/Co3/Cu4.5/Co1/Py3/Co1/substrate have similar structure, and only the position of the Co NOL was different. NOL on either the top or bottom position gives the same frequency response on MI. Clearly, the $\mathrm{NOL_{top}}$/PSV/$\mathrm{NOL_{bottom}}$ has higher capacitance and hence gave the larger capacitance than the PSV with either the top or bottom NOLs.

It is interesting that the obvious change of the Im (Z) curves was found when the $\mathrm{NOL_{bottom}}$ and the $\mathrm{NOL_{top}}$ were different oxidized materials, such as Co and Ta, with the same oxidation process, as shown in Fig. 5. That the Im (Z) curves were separated obviously indicated that these PSVs with different capacitances. The $f_r$ of the PSV with the Ta $\mathrm{NOL_{bottom}}$ and the PSV with the Co $\mathrm{NOL_{top}}$ is 30 and 37.5 kHz, respectively. This indicates that the capacitance effect of the Ta $\mathrm{NOL_{bottom}}$ is larger than that of the Co $\mathrm{NOL_{top}}$. In general, Co is more easily oxidized than Ta because the condensed $\mathrm{TaO_X}$ on the surface of Ta would prevent the Ta under the $\mathrm{TaO_x}$ from following oxidation. Then, during the same oxidation time, the thickness of the Co $\mathrm{NOL_{top}}$ is thicker than that of the Ta $\mathrm{NOL_{bottom}}$. Therefore, the $f_r$ of the PSV with the Co $\mathrm{NOL_{top}}$ is larger than that of the PSV with the Ta $\mathrm{NOL_{bottom}}$. The $f_r$ of the PSV with double NOLs is 7.6 kHz. Obviously, the double NOLs has the largest effective capacitance, which is contributed from the $\mathrm{NOL_{top}}$ and the $\mathrm{NOL_{bottom}}$, and thus the smaller $f_r$.

## IV. Conclusion

We have demonstrated the analysis of a $\mathrm{NOL_{top}}$/PSV/$\mathrm{NOL_{bottom}}$ system using magnetoimpedance spectroscopy. Since any change of capacitance caused by variation of NOL would result in the shift of roll-off frequency, the roll-off frequency is linear to the NOL thickness and showed the reverse proportion to the $C_{\mathrm{eff}}$ and calculated $C_{\mathrm{NOL}}$ when the bottom Py layer was fully oxidized. By this nondeconstructive impedance spectroscopy analysis method, the properties of the NOL in PSV could be easily distinguished.

## Acknowledgment

This work was supported in part by the National Science Council under Grant NSC 94-2120-M-001-004 and in part by the Ministry of Economic Affairs under Grant A341XS3219.

## References

[1] N. Baibich, J. M. Broto, A. Fert, F. Nguyen Van Dau, F. Petroff, P. Creuzet, A. Friederich, and J. Chazelas, "Giant Magnetoresistance of (001) Fe/(001)Cr Magnetic Superlattices," *Phys. Rev. Lett.*, vol. 61, pp. 2472–2475, 1988.

[2] B. Dieny, V. Speriosu, B. Gurney, S. Parkin, D. Wilhoit, K. Roche, S. Metin, D. Peterson, and S. Nadimi, "Spin-valve effect in soft ferromagnetic sandwiches," *J. Magn. Mag. Mater.*, vol. 93, pp. 101–104, 1991.

[3] M. Mao, C. Cerjan, and J. Kools, "Physical properties of spin valve films grown on naturelly oxidized metal nano oxide surfaces," *J. Appl. Phys.*, vol. 91, pp. 8560–8562, 2002.

[4] M. F. Gillies, A. E. T. Kuiper, R. Coehoorn, and J. J. T. M. Donkers, "Compositional, structural, and electrical characterization of plasma oxidized thin aluminum layers for spin-tunnel junctions," *J. Appl. Phys.*, vol. 88, pp. 429–434, 2000.

[5] T. Y. Peng, L. C. Hsieh, W. C. Chien, C. K. Lo, Y. W. Huang, S. Y. Chen, and Y. D. Yao, "Impedance behavior of spin valve transistor," *J. Appl. Phys.*, vol. 99, p. 08H710, 2006.

[6] *Impedance Measurement Handbook*, Agilent Technol., Palo Alto, CA, 2003, pp. 2–18. K. Okada, T. Sekino.

[7] H. Kaiju, S. Fujita, T. Morozumi, and K. Shiiki, "Magnetocapacitance effect of spin tunneling junctions," *J. Appl. Phys.*, vol. 91, pp. 7430–7432, 2002.

[8] M. F. Gillies, A. E. T. Kuiper, R. Coehoorn, and J. J. T. M. Donkers, "Compositional, structural, and electrical characterization of plasma oxidized thin aluminum layers for spin-tunnel junctions," *J. Appl. Phys.*, vol. 88, pp. 429–434, 2000.

Manuscript received March 13, 2006 (e-mail: w_c_jian@alumni.ccu.edu.tw)